Hydrol. Earth Syst. Sci. Discuss., 10, 9575–9613, 2013
www.hydrol-earth-syst-sci-discuss.net/10/9575/2013/
doi:10.5194/hessd-10-9575-2013

Hydrology and Earth System Sciences
Open Access
Discussions

A large-scale, high-resolution hydrological model parameter dataset for climate change impact assessment for the conterminous United States

A. A. Oubeidillah[1], S.-C. Kao[1], M. Ashfaq[1], B. Naz[1], and G. Tootle[2]

[1]Oak Ridge National Laboratory, Oak Ridge, TN, USA
[2]University of Alabama, Tuscaloosa, AL, USA

Received: 2 July 2013 – Accepted: 10 July 2013 – Published: 22 July 2013

Correspondence to: S.-C. Kao (kaos@ornl.gov)

Published by Copernicus Publications on behalf of the European Geosciences Union.

Abstract

To extend geographical coverage, refine spatial resolution, and improve modeling efficiency, a computation- and data-intensive effort was conducted to organize a comprehensive hydrologic dataset with post-calibrated model parameters for hydro-climate impact assessment. Several key inputs for hydrologic simulation, including meteorologic forcings, soil, land class, vegetation, and elevation, were collected from multiple best-available data sources and organized for 2107 hydrologic Subbasins (HUC8s) in the conterminous US at refined 1/24° (~ 4 km) spatial resolution. Using high performance computing for intensive model calibration, a high-resolution parameter dataset was prepared for the macro-scale Variable Infiltration Capacity (VIC) hydrologic model. The VIC simulation was driven by DAYMET daily meteorological forcing and was calibrated against the USGS WaterWatch monthly runoff observations for each HUC8. The results showed that this new parameter dataset may help reasonably simulate runoff at most of the US HUC8 Subbasins. Based on this exhaustive calibration effort, it is now possible to accurately estimate the required resources for further model improvement across the entire conterminous US. We anticipate that through this hydrologic parameter dataset, the repeated effort of fundamental data processing can be lessened, so that research efforts can be emphasized on the more challenging climate change impact assessment.

1 Introduction

With the advance of high performance computing and more abundant historic observation, hydrologists and water resource engineers are now better equipped to improve the scale, resolution, and accuracy of hydrologic simulation. Depending on the need, a suitable hydrologic model may range from a statistical model (e.g., artificial neural network, ANN) or conceptual model (e.g., bucket model), to a more sophisticated model that can simulate a series of hydrological processes based on physical mechanisms. However,

HESSD
10, 9575–9613, 2013

although a statistical model can generally simulate hydrologic variables well with fewer predictors, the assumption of stationarity may be questionable in a changing environment in which many hydrologic processes are expected to be disrupted (Milly et al., 2008). Under such conditions, historic relationships may not provide fully accurate information about future streamflow and water availability. One example is ANN (and the various related machine learning algorithms). Although these types of advanced statistical methods are extremely powerful in forecasting reservoir outflows with minimal observation, the physical relationships among various predictors can hardly be interpreted (Govindaraju and Rao, 2000); this hinders the direct extension across different locations and climate patterns. Therefore, these methods may not be suitable choices for climate-related research.

Unlike statistical models, process-based models are theoretically justifiable for climate research. Since most hydrologic mechanisms are simulated through deterministic laws, the assumption of stationarity is less an issue. However, a high number of observations and parameters are required to drive process-based models. For instance, a distributed rainfall–runoff model may require fine-resolution inputs of vegetation, precipitation, temperature, solar radiation, topography, and many other soil properties to simulate various hydrologic processes such as evapotranspiration, infiltration, vegetation root absorption, snowmelt, and runoff generation. With increasing complexity in model resolution, scale, and processes, the required computational resources also increase exponentially. As a result, it is generally more challenging to conduct process-based hydrologic simulation for a large study area with fine spatial resolution. A tradeoff usually must be made between scale and resolution because of resource limitations.

Numerous studies have investigated the hydrological impacts of climate change in the US using process-based models (Mote et al., 2005; Christensen et al., 2004; Payne et al., 2004; Maurer, 2002; McCabe and Hay, 1995; Hamlet and Lettenmaier, 1999; Wolock and McCabe, 1999; Ashfaq et al., 2010). Output from global climate model (GCM) is usually downscaled, bias-corrected, and used in conjunction with hydrologic models to assess future water availability. However, owing to resource limitations, many

HESSD
10, 9575–9613, 2013

hydro-climate impact assessments either are focused on smaller US regions or provide lower spatial resolution (Christensen et al., 2004; Payne et al., 2004; Maurer et al., 2002; McCabe and Hay, 1995). Repeated efforts may be needed for fundamental data processing and model calibration, and these may unavoidably shrink the amount of attention available for the more challenging climate change impact assessment. To extend geographical coverage, refine spatial resolution, and make hydro-climate impact assessment more efficient, a comprehensive set of calibrated physical parameters is desired that can provide the most up-to-date, high-resolution watershed soil, vegetation, elevation, and other hydrologic characteristics. If a fine-resolution hydrological model parameter dataset could be pre-organized, generally calibrated and constantly updated, it would enable numerous researchers to easily extend hydro-climate impact assessment efforts to different watersheds.

One major structural difference between climate and hydrologic models is their respective requirements for vertical and horizontal resolution. GCMs can be coarser in spatial resolution, but they need more vertical layers to better simulate boundary layer and tropospheric processes that govern complex land–atmosphere–ocean interactions at varying time-scales. However, horizontal resolution is the dominant factor for hydrologic models, since complicated topography and heterogeneous land surface characteristics have the greatest impacts on model performance. Shrestha et al. (2006) found that finer-resolution data input would result in better model performance in comparing simulated and observed discharge at different model resolutions. Therefore, to enhance the performance of hydrologic simulations for climate change impact assessment, one would need to simultaneously improve both spatial resolution (for hydrologic research needs) and geographical coverage (for climate change research needs). With the continuous improvement of spatial resolution through regional climate models (e.g., North American Regional Climate Change Assessment Program (NARCCAP) and Coordinated Regional climate Downscaling Experiment (CORDEX)), the refined climate projections will soon become available. The corresponding enhancement of hydrologic models is hence required for detailed hydro-climate impact assessment.

HESSD
10, 9575–9613, 2013

Given the motivation, a data- and computation-intensive effort was performed in this study. Using multiple state-of-the-art geospatial datasets for the conterminous US, various key hydrologic model inputs, including topography, soil characteristics, vegetation, land surface classification, meteorological forcing and runoff observation were organized in a nationally consistent 1/24° (~ 4 km) grid and grouped by the US Geological Survey (USGS) 8-digit hydrologic unit (HUC8 or Subbasin; Seaber et al., 1987). The refinement from commonly-used 1/8° (~ 12 km) resolution (e.g., Maurer et al., 2002; Mitchell et al., 2004) will allow more flexibility to characterize detailed hydrologic responses. A widely used hydrologic model, Variable Infiltration Capacity (VIC), was chosen as the baseline hydrologic model in this initial effort. A parallelization scheme was developed for each of the 2107 HUC8 Subbasins to greatly reduce the required computation time. Using high performance supercomputing, an exhaustive model calibration exercise was then performed to improve the model accuracy across the conterminous US. The calibrated model was evaluated using USGS observed runoff, and it showed that the parameter dataset may provide satisfactory skills for most of the US HUC8 Subbasins. In Sect. 2, the data source and methodology used to develop the parameter datasets are described. The current model performance is presented in Sect. 3, and a summary and conclusions are provided in Sect. 4.

2 Data and methodology

2.1 Study area and assessment grids

The effect of spatial resolution on hydrologic modeling is illustrated in Fig. 1 for the Ashley–Brush Subbasin in Utah (HUC8 ID 14060002). Based on the 1/3 arcsec-resolution (~ 10 m) USGS national elevation dataset (NED; Gesch et al., 2002), the average elevation was computed for both 1/24° (~ 4 km) and 1/8° (~ 12 km) grids. Flow direction and flow accumulation were then derived using standard geographical information system (GIS) software. Grids with flow accumulation values greater than 20 in Fig. 1a and

HESSD
10, 9575–9613, 2013

greater than 2 in Fig. 1b are marked in grey, illustrating the locations of rivers seen by computer models. Three USGS gauge stations (09261700, 09263500, and 09271550) are also marked in Fig. 1. Whereas the 4 km grids can capture two streams, the 12 km grids fail to depict the system. Without additional information, the hydrological model might consider both outlets (09263500 and 09271550) as being located on the same river, which would directly affect the model calibration and validation. In addition, most of the 12 km grids flow to the neighboring Subbasin instead of to the two outlets because of the insufficient spatial resolution for this watershed.

Therefore, to refine hydro-climate assessment from regional to watershed scale, spatial resolution is a key. After evaluating the available resource, it was decided to select 4 km as the targeted resolution, which requires more than 10 times of computation resources comparing to the commonly-used 12 km grids. The 4 km grids selected herein in fact follow the same configuration as the Parameter-elevation Regressions on Independent Slopes Model meteorological datasets (PRISM; Daly et al., 2002), with the north boundary extending to 53° N to cover the entire Columbia River basin on the Canadian side. Since PRISM is recognized as the most accurate grid-based monthly meteorological observation of precipitation and temperature, it is convenient to use the same grid configuration for future model evaluation and comparison. Each 4 km grid was given a unique identifier and further labeled with USGS HUC8 IDs. The watershed boundary outside the conterminous US was obtained from the USGS National Hydrography Dataset Plus, version 1 (NHDPlus; EPA/USGS, 2010). Overall, there are ~ 480 000 grid points and 2107 HUC8s in 18 hydrologic Regions (HUC2) in the conterminous US. HUC2 and HUC8 are illustrated in Fig. 2.

2.2 Meteorological forcing

"Meteorological forcing" refers to the required meteorological inputs for hydrologic modeling, including precipitation, temperature, wind speed, and others. Conventionally, these values are looked up from gauge observations (e.g., National Weather Service Cooperative Observer Program) and then spatially interpolated for further hydrologic

HESSD
10, 9575–9613, 2013

application. However, given the heavy data processing requirements, such an approach is not applicable for large-scale hydrologic simulation; therefore, pre-processed grid-based observations are primarily used.

Currently, several meteorological forcing datasets are commonly used in hydrologic studies for the conterminous US. These datasets are either fully based on gauge observation or partially assimilated through weather forecasting models. By considering the topographical effect and some other adjustment factors, PRISM is recognized as the most accurate grid-based observation of precipitation and temperature. PRISM is available on a monthly time scale from 1895 to the present and is in 1/24° (~ 4 km) spatial resolution. Maurer et al. (2002) is a widely used forcing dataset for hydrologic studies. It is based on gauge observation and is available on a daily time scale from 1950 to the present in 1/8° (~ 12 km) spatial resolution. Targeted for fine-scale ecological studies, DAYMET (Thornton et al., 1997) is another commonly used meteorological dataset based on observation (White et al., 2006; Keane et al., 2008; Manter et al., 2005). DAYMET is available on a daily time scale from 1980 to the present at a projected 1 km spatial resolution. The North American Regional Reanalysis (NARR; Mesinger et al., 2006) is an assimilated meteorological reanalysis dataset that provides a complete set of meteorological variables (e.g., pressure, wind). NARR is available on a 3 h time scale from 1979 to the present at a 36 km horizontal grid spacing. Some other new meteorological forcing datasets are also available (e.g., Abatzoglou, 2013).

To support further model calibration and application, the four datasets mentioned (PRISM, Maurer, DAYMET, and NARR) were processed in a consistent format on the 4 km grids described in Sect. 2.1. Spatial interpolation was performed for both Maurer and NARR from 1/8° and 36 km to 1/24° (~ 4 km) for direct comparison. The 3 h wind speed from the lowest layer in NARR was used to calculate mean daily wind speed for comparison with the wind speed provided by Maurer. Spatial aggregation was performed for DAYMET to gather information from 1 km to 1/24° (~ 4 km) horizontal grid spacing. Overall, daily precipitation and minimum and maximum temperatures are available from 1980 to the present for Maurer, DAYMET, and NARR; but daily wind

HESSD
10, 9575–9613, 2013

speed is available only for Maurer and NARR. An overall comparison is presented in Sect. 3.1. Since it was not possible to fully judge which dataset would be the closest to actual observations, DAYMET was chosen as the default meteorological dataset in this study, given its finer spatial resolution (i.e., aggregation is considered to be more justifiable than interpolation). For non-US regions in which DAYMET is unavailable, NARR information was used.

2.3 Soil parameters

Soil parameters are mainly used to describe the process of infiltration and baseflow generation in hydrologic modeling. Given their heterogeneous nature and the lack of an effective remote sensing method, soil parameters remain most uncertain of all parameters. Intensive hydrological model calibration is usually performed on soil parameters to improve the overall model performance. In this initial effort, the Conterminous US Soil dataset (CONUS-SOIL; Miller and White, 1998) was used to provide the required soil information for hydrologic modeling. CONUS-SOIL was derived from the State Soil Geographic dataset (Schwarz and Alexander, 1995). It provides commonly used soil characteristics arranged in 11 standard layers ranging from 0 to 2.5 m in depth and is specifically aimed at hydro-climate applications. The CONUS-SOIL dataset is available in 1 km spatial resolution and is provided in common GIS formats (e.g., raster or polygon). Each CONUS-SOIL grid is spatially joined to the 4 km grids (described in Sect. 2.1) so that the required soil characteristics can be summarized efficiently for further hydrologic application. Future effort will be invested in collecting soil characteristics for non-US regions that are not covered by CONUS-SOIL.

2.4 Vegetation parameters

In considering the water budget for a large study domain, uptake and evapotranspiration from vegetation is a critical factor, since it has a significant influence on the seasonality of the simulated hydrology. Because of the rapid improvement in remote

HESSD
10, 9575–9613, 2013

sensing data over the past decade, historic surface vegetation can now be more effectively captured to support large-scale hydro-climate simulation.

In this study, both the University of Maryland (UMD) land cover classification (Hansen et al., 2000) and NASA Moderate Resolution Imaging Spectroradiometer (MODIS) model 15A2 Leaf Area Index (LAI) information were imported. The UMD land cover classification consists of 14 categories of vegetation (e.g., evergreen needleleaf forest, mixed forest) and is available at 1 km spatial resolution in GeoTIFF format. To link the 1 km land cover classification to the 4 km grids used in this study, a conversion table for these two grid systems was developed. Both grids were first converted to polygons and then spatially intersected to form a massive table that contains the overlapping surface area of each spatial unit and the unique identifiers from both datasets. This massive conversion table was then used to summarize the portion of the UMD land cover classification in each 4 km grid efficiently.

To capture the seasonal pattern of surface vegetation, the MODIS15A2 LAI was included. LAI, defined as the green leaf area per unit of ground area (leaf area/ground area), is a widely used dimensionless canopy index. Depending on the type of vegetation, LAI may show significant seasonal trends. By using the MODIS remote sensing data, the historic time series of LAI were constructed. The MODIS15A2 information is available every 8 days and is stored in HDF format, approximately 1 km spatial resolution in sinusoidal projection. For consistency with the UMD land classification, the MODIS LAI values were spatially interpolated to the UMD 1 km grids. The interpolated 8 day LAI values were then aggregated for each month and linked to the 4 km grids via the same conversion table developed for the UMD grids. Overall, the monthly LAI time series are organized from 2003 to the present and can be used to support various hydrologic applications. The overall statistics are summarized in Sect. 3.2.

2.5 Elevation and topography

Elevation and topography have a significant influence on surface hydrology. For instance, slope directly affects flow velocity, and local topographical depressions may

HESSD
10, 9575–9613, 2013

create impoundments and delay surface runoff. Snow accumulation and snowmelt are also closely related to elevation. To refine the spatial resolution of a hydro-climate assessment, a fine-resolution elevation dataset is needed. In this study, the 1/3 arcsec-resolution (~ 10 m) USGS NED (Gesch et al., 2002) was used for the conterminous US. NED is a seamless dataset with the best available raster elevation data in the US. Similar to the treatment of UMD grids, each NED grid was labeled with a unique 4 km grid identifier. Average elevation, average slope, and the histogram of the elevation at each 4 km grid were then computed. For regions outside the US, the 90 m Shuttle Radar Topography Mission elevation was used instead (Farr et al., 2007). The pre-organized information can be processed efficiently for further applications.

2.6 Observed streamflow and runoff

Historic hydrologic observations are required for model calibration and validation. Two types of observations, streamflow and runoff, can be used to support hydrologic model calibration. Gauge-based streamflow observations directly measure flow discharge at a specific river section. Comprehensive daily flow observations can be obtained from the USGS National Water Information System (NWIS) for more than 22 000 current and retired gauge stations throughout the US.

Another observational product, the USGS WaterWatch runoff (Brakebill et al., 2011), was found to be more useful in this study. Derived from the comprehensive NWIS gauge observation, WaterWatch runoff is the assimilated time series of flow per unit of area calculated for each conterminous HUC8 Subbasin. For each HUC8 Subbasin, multiple NWIS gauge stations located within or downstream of the HUC8 were used to estimate the runoff generated locally at each HUC8. The contributing drainage areas (both gauge-to-HUC8 and HUC8-to-gauge) were converted as weighting factors to merge runoff time series from all stations. As a result, gauges with drainage coverage most similar to that of the particular HUC8 received the highest weights. Therefore, the influence of highly regulated gauge stations (usually with large drainage coverage across multiple HUC8s) could be reduced. This approach may effectively assimilate

HESSD
10, 9575–9613, 2013

streamflow observations from multiple gauge stations as a consistent areal HUC8 runoff measurement that has a unit similar to that for precipitation (depth/time). WaterWatch runoff is available monthly from 1901 to the present. Note that the WaterWatch runoff is based on an earlier version of watershed boundaries and was found to be slightly different from the new watershed boundaries adopted in Sect. 2.1. Using the polygon shapefiles from both versions of the watershed boundaries, a conversion table based on overlapping drainage areas was developed to adjust the WaterWatch runoff to a consistent watershed boundary for further comparison.

2.7 Baseline hydrologic model application

In this study, the widely-used VIC model (Nijssen et al., 1997; Liang et al., 1994, 1996; Cherkauer et al., 2002) was selected as the baseline hydrologic model application for the conterminous US. VIC model has been successfully tested in a wide number of hydrologic studies and a number of large river networks (Gao et al., 2010; Ashfaq et al., 2010; Su et al., 2005; Nijssen et al., 1997, 2001; Bowling et al., 2004; Lohmann et al., 1998). The current VIC model studies were mostly conducted at 1/8° spatial resolution (~ 12 km). Given its wide acceptance and the fact that it can be directly implemented for parallel computing, VIC model was considered the most suitable baseline hydrologic model for this initial effort. VIC model is a process-based hydrological model that simulates evapotranspiration, snow pack, surface runoff, baseflow and other hydrologic mechanisms at daily or subdaily time steps. The water and energy balance are solved for multiple elevation bands and vegetation types, which allows the model to capture the subgrid-scale variability of these land surface features. The model simulates all processes in each grid cell independently, in an equally spaced grid. The infiltration and runoff are estimated using the VIC model curve, which uses the soil moisture content of the upper two soil layers to approximate the spatial variability of surface saturation. The empirical Arno curve is used to generate base flow based on the soil moisture content in the bottom layer (Cherkauer et al., 2003). A routing algorithm external to

HESSD
10, 9575–9613, 2013

the VIC model can then be used to simulate the streamflow at a specified location by routing runoff and baseflow from each grid cell (Lohmann et al., 1998).

VIC model requires a large number of parameters, including soil, vegetation, elevation, and daily meteorological forcings, at each grid cell. By taking daily precipitation, maximum/minimum temperature, and wind speed as inputs, VIC model computes potential evapotranspiration through the Penman Monteith equation (see Maidment, 1993). Other forcings, including short-wave and long-wave radiation, relative humidity, and vapor pressure, are estimated by using algorithms from MTCLIM (Kimball et al., 1997; Thornton and Running, 1999) at subdaily time steps (3 h). Additionally, 3 h temperatures are estimated within the model as a parameterization of maximum/minimum temperature (Bohn et al., 2013).

For soil physical properties, the CONUS-SOIL information was divided into three layers covering the total depth from 0 to 2.5 m (CONUS-SOIL layers 1 and 2 to VIC model layer 1, CONUS-SOIL layers 3–7 to VIC model layer 2, and CONUS-SOIL layers 8 and 9 to VIC model layer 3). The 1 km CONUS-SOIL information was then aggregated to 4 km grids. When a 3-layer configuration was used, a total of 53 soil parameters was required, including saturated hydrologic conductivity, initial soil moisture, bulk density, layer thickness, fraction of soil moisture at wilting point, and some other conceptualized parameters like the variable infiltration curve parameter (b_{infilt}), which required further calibration. Although CONUS-SOIL contains a number of different soil characteristics, only a few are directly called out in the VIC model soil parameter file (e.g., bulk density). Most VIC model soil parameters are derived from porosity and soil texture class according to a standard index table provided by the VIC modeling group. A few other non-soil parameters requested in the soil parameter file – such as the average annual air temperature, average annual precipitation, average elevation, and slope (used to derive the maximum velocity of the baseflow) – were derived from DAYMET and NED. If the CONUS-SOIL information was totally unavailable for a specific grid point, the information from the nearest grid point was used instead.

HESSD
10, 9575–9613, 2013

The VIC model vegetation parameter file describes the number and percentage of vegetation types in each grid cell. The conversion table described in Sect. 2.4 was used to efficiently summarize the UMD vegetation classification to the format requested by VIC model. To improve the characterization of surface vegetation, a data-intensive enhancement was applied to import the monthly LAI observation from MODIS at each 4 km grid. The monthly LAI was first computed from the 2003–2008 MODIS at each 1 km UMD grid and then converted to the subgrid vegetation information in the VIC model format. Although the time frame between UMD (before 2000) and MODIS LAI (2003–2008) is somewhat inconsistent, given that there is no suitable alternative, both datasets are considered to be the best proximity for the actual vegetation class and LAI.

To better represent snow accumulation and snowmelt, the subgrid elevation band information can be set up (i.e., fractions of the grid area with their corresponding mean elevations). Since NED provides a much finer spatial resolution (10 m) than the 4 km grid, the subgrid elevation band can be described in high detail. However, the elevation band should also be considered in terms of the required computation resources. It was found that the required computational time is roughly proportional to the number of elevation bands; therefore, in some flat regions, it might not be worthwhile to use multiple bands. For flexibility, instead of creating elevation bands at fixed intervals, the histogram of elevation at each 4 km was summarized. Depending on the required research question and the available resources, a suitable number of elevation bands can be generated in the VIC model format efficiently.

2.8 Calibration through high-performance computing

Although the process-based models incorporated various explicit physical mechanisms, given the complexity of hydrologic phenomena, parts of the processes still replied on conceptual statistical parameterization. As a result, several non-physically-based parameters would require further calibration before a model could be put to use. Calibration was also required for those parameters with high measurement uncertainty

HESSD
10, 9575–9613, 2013

(e.g., most of the soil parameters), since they may affect the performance of hydrologic modeling significantly. Nevertheless, a full hydrologic calibration is extremely resource-intensive, especially when the model application requires fine resolution and sophisticated mechanisms. Using state-of-the-art high performance computation, we performed a first-order modeling calibration for each HUC8 consistently through a computationally exhaustive algorithm to improve the overall model performance. This large-scale calibration was mainly targeted at narrowing the possible range of suitable parameter values in each HUC8. Depending on the needs of future research, further fine calibration can be performed efficiently.

Following the sensitivity analysis by Demaria et al. (2007), five sensitive VIC model parameters were selected for calibration, including the variable infiltration curve parameter (b_{infilt}), exponent of the Brooks–Corey drainage equation (exp), thickness of soil layer 2 (thick_2), fraction of the maximum velocity of baseflow where nonlinear baseflow begins (Ds), and fraction of maximum soil moisture where nonlinear baseflow occurs (Ws). Although other VIC model parameters could also be important (e.g., thickness of soil layer 3, thick_3), they were not considered in the current effort given the computational resource limitations. Although the soil parameters were obtained with a prespecified soil depth, the thickness of soil layer 2 (root layer) was treated as a parameter and can be changed during calibration. Given that the USGS WaterWatch runoff can provide an estimate of local runoff at each HUC8, our calibration was performed by matching the simulated total monthly runoff (baseflow + surface runoff) to the observed WaterWatch monthly runoff. In other words, the off-line routing model was not used, a decision similar to Demaria et al. (2007). For each parameter, three combinations, including the upper and lower bounds and the suggested default values, were chosen for calibration (Table 1). A total of 243 (3^5) parameter scenarios were then prepared. The VIC model simulation was driven by DAYMET daily meteorological forcing (precipitation and minimum/maximum temperature) and NARR daily wind speed from 1980 to 2008. Year 1980 was treated as the model startup period, 1981–2000 as the calibration period, and 2001–2008 as the validation period. The VIC model simulation

HESSD
10, 9575–9613, 2013

was performed in 3 h time steps using the energy and water balance mode. VIC version 4.1.1 was used in the current study, and the recently-released VIC 4.1.2 will be incorporated after the model development work has been stabilized.

To effectively manage the data flow, all forcing, soil, vegetation, global parameter, and output flux files were organized in separate HUC8 folders. Depending on the total watershed area, all grid points within a HUC8 were subdivided into 16, 32, or 48 computation units. Each computational unit had separate global, soil, vegetation, and elevation parameter files and could be executed independently. Computation was performed using Oak Ridge National Laboratory's Titan supercomputer, a Cray XK7 system with 18 688 computational nodes, each equipped with four quad-core CPUs and two GPU cards. The extensive simulation exhausted ~ 1.5 million CPU-hours (i.e., the number of CPUs multiplied by the average hours used by each CPU), approximately 171 calendar years if done by a single-core desktop machine. Note that although we had planned to use a 10-layer elevation band during calibration, that would have resulted in a huge increase in the required computational time (an estimated 15 million CPU-hours, approximately) over our allowable resource. Given that the current calibration was targeted for total monthly runoff and was less affected by the elevation band, a one-layer elevation band was used. When hydro-climate projections are produced for future research, multiple elevation bands will be implemented.

Four statistical matrices, the coefficient of determination (R^2), Nash–Sutcliffe model efficiency coefficient (Nash), mean absolute error (MAE), and root mean square error (RMSE), were used to evaluate model performance. The matrices are summarized in Table 2, in which O_t and Y_t represent the observed and modeled monthly total runoff from month 1 to n, and $\overline{O}$ and $\overline{Y}$ represent the mean of O_t and Y_t. For each HUC8, daily total runoff was computed by summing baseflow and surface runoff at each 4 km grid and then aggregated up to calculate the HUC8 monthly runoff (Y_t). The observed monthly runoff (O_t) from the USGS WaterWatch was then used for model evaluation. In addition to runoff analysis, the simulated 1 April snow water equivalent (SWE) was also compared to the snow course observations. The results are reported in Sect. 3.4.

HESSD
10, 9575–9613, 2013

3 Results and discussions

3.1 Difference among forcing datasets

To understand the difference among four selected forcing datasets (Maurer, PRISM, DAYMET and NARR), an overall comparison was performed (illustrated in Fig. 3). Average daily maximum temperature (T_{max}), daily minimum temperature (T_{min}), annual total precipitation (P), and average wind speed (W) from 1980 to 2008 for each of the 2107 HUC8s were computed for comparison. The correlation coefficients among the HUC8 average values were also computed. Given that PRISM is considered to be the most accurate monthly observation, it is placed in the x-axis as the target for comparison. Figure 3a illustrates the difference for T_{max}. Although both Maurer and DAYMET are close to the PRISM observation, NARR seems to be warmer in most of the HUC8s. The difference is not as significant for T_{min} in Fig. 3b, where most of the datasets are similar to each other, with NARR slightly warmer than the DAYMET and Maurer datasets. A consistent observation can be made for the difference of P in Fig. 3c. Both DAYMET and Maurer are closer to PRISM, but NARR is more divergent than the other datasets. Given that wind speed is available only for Maurer and NARR, only one set of points are plotted in Fig. 3d. A significant difference can be seen in the two datasets, with a correlation coefficient of around 0.28. To understand the difference, the geographical wind speed patterns are further plotted in Fig. 4. Clearly, the inconsistency should be from the differences in the original data sources. The wind speed provided in Maurer's dataset was calculated from the coarser-resolution reanalysis dataset and hence shows a smoother pattern in Fig. 4b. Given that NARR can provide a more delicate local wind spend pattern, the NARR wind speed was chosen as the default wind speed in this study.

HESSD
10, 9575–9613, 2013

3.2 Monthly and annual statistics of LAI

To examine the variability of the MODIS leaf area index, the monthly and annual average LAI are plotted in Fig. 5. For each UMD class, the mean monthly MODIS LAI values were calculated for the entire conterminous US from January 2003 to December 2008. The monthly average LAI values are shown in Fig. 5a, in which the highest LAI values are found for Evergreen Broadleaf, Deciduous Broadleaf, and Mixed Forest, and the lowest LAI values in Bare Ground, Open Shrubland, and Closed Shrubland. In terms of seasonal pattern, the LAI values for Evergreen Broadleaf are consistently high across all seasons. Both Deciduous Broadleaf and Mixed Forest have the strongest seasonal variation and can be larger than Evergreen Broadleaf during summer. The annual averages are plotted in Fig. 5b, which shows that the annual variability is not significant at the conterminous US scale. Therefore, it should be justifiable to generate VIC vegetation parameters by averaging the LAI values from 2003 to 2008. It is interesting to note that the LAI values reported in the Urban and Built land class are not among the smallest. Those results may be explainable by considering that the findings are based on 1 km grid resolution, and at that resolution, many suburban areas are still covered by plants.

3.3 Difference between runoff aggregation and routing

To simulate streamflow in the VIC model, a separate routing model developed by Lohmann et al. (1998) was required. The routing model simulated a channel network with a number of nodes, each of which represented information from a grid cell. A unit hydrograph was then used to route the simulated surface runoff and baseflow through a channel network using a linearized St. Vennant's equation (Lohmann et al., 1998). The routing model required five types of input: flow direction, grid area fraction, flow velocity, watershed boundary mask, and gauge locations. Whereas flow direction, grid area fraction, and watershed boundary can be derived from digital elevation models, flow velocity and unit hydrograph involve larger uncertainty and cannot be easily

HESSD
10, 9575–9613, 2013

estimated. As discussed in Sect. 2.1, the resolution of digital elevation models also has a significant influence on the accuracy of river networks.

Although the major purpose of a routing model is to account for the travel time of river flow, this step may reasonably be skipped in smaller watersheds (i.e., when travel time is short) by using a simpler runoff aggregation method (Demaria et al., 2007). To evaluate the difference, a comparative analysis was performed for two randomly selected USGS gauge stations. Both gauge 01047000 in HUC01030003 and 02342500 in HUC03130003 are under little or no anthropogenic disruption and have complete records from 1980 to 2008. Routing models were set up to calculate streamflow at these two gauge stations. The simulated total monthly runoff (surface runoff + baseflow) and monthly average streamflow are illustrated in Fig. 6, with runoff observations taken from WaterWatch and gauge observations from NWIS. The correlation coefficient (ρ) between the observed and simulated runoff/streamflow was also calculated.

Generally speaking, the model performance showed large similarities for both approaches, with correlation coefficients between simulation and observation varying from 0.8 to 0.9. Although the travel time was not modeled in the runoff aggregation approach, the extra uncertainty induced by the routing model was also avoided (e.g., flow speed, routing resolution), so pros and cons exist for both methods. Given that our main objective was to provide a first-order calibrated hydrological parameter dataset to expedite further efforts at fine calibration, it is more efficient and consistent to calibrate VIC for each HUC8 through the runoff aggregation approach. Also, since it is extremely time-consuming to develop reasonable routing models for all HUC8s in the US, the runoff aggregation approach provides an easier alternative than spatially examining the model performance for a great number of watersheds in the US.

3.4 Overall model performance

Overall model performance is illustrated in Fig. 7. For each HUC8, the WaterWatch observed and VIC simulated total annual runoff (baseflow + surface runoff) are computed

HESSD
10, 9575–9613, 2013

for both calibration and validation periods. The correlation coefficients between observed and simulated HUC8 annual runoff are 0.954 in the calibration period and 0.940 in the validation period, which is satisfactory overall. The results represent an improvement from 0.906 using an uncalibrated 4 km dataset (i.e., with default parameters) and from 0.877 using an uncalibrated 12 km dataset, both with a much larger spread (note: uncalibrated results were not illustrated in this paper).

In Fig. 7, it can be seen that the current parameter sets overestimate runoff in multiple drier HUC8s. To spatially examine the model performance for the entire conterminous US, the observed and simulated annual runoff, R^2, Nash, MAE, and RMSE for each HUC8 are illustrated in Fig. 8. The median values of the HUC8 evaluation matrices in each hydrologic region are also summarized in Table 3. From Fig. 8a and b, it can be seen that VIC model generally captures the spatial patterns of WaterWatch runoff. However, the simulated runoff is higher in many HUC8s, especially in very dry regions such as the Rio Grande (HUC 13), Lower Colorado (HUC 15), Texas (HUC 12), Great Basin (HUC 16), and Arkansas–White–Red (HUC 11). To enable a closer look, both R^2 (Fig. 8c) and Nash (Fig. 8d) between the observed and simulated monthly runoff are illustrated. Clearly, while the current parameter sets may provide satisfactory results for wetter regions, it is challenging to capture the monthly runoff time series in drier regions. Further studies in dry regions are required, since the suitable parameter values and model setup may have exceeded the currently suggested ones. This issue may be also related to meteorological forcing. It was noticed that DAYMET generally provided higher precipitation (~ 25 % greater than PRISM) in dry HUC8s; and under such situation, the VIC model cannot be further imporved unless reducing precipaition portionally to the PRISM values. Nevertheless, since these regions are fairly dry, they in fact have smaller MAE (Fig. 8e) and RMSE (Fig. 8f) compared to other wet regions. Therefore, the overall impact of wet-bias in drier regions may not be significant since they are on a much smaller scale.

To evaluate the model performance for other variables, the simulated 1 April SWE was compared to the observed snow course data used by Mote et al. (2005). Focusing

HESSD
10, 9575–9613, 2013

on the 1981–2000 period, 784 snow stations with complete annual 1 April SWE observation were selected. For each station, simulated 1 April SWE at the nearest grid was looked up. Since the point observation may be in a different scale than the grid-based SWE, correlation coefficient between observation and simulation is computed for evaluation. The results are summarized in Fig. 9. In Fig. 9a, the histogram of ρ is plotted, and it shows that high correlation coefficients can be seen in most of the stations. To examine the statistical significance, the histogram of P value is plotted in Fig. 9b. Since P value is less than 0.05 for nearly 700 stations (i.e., correlation is statistically significant under 5 % significance level), it suggests that the simulation may capture the annual trend for most of the stations. To check the spatial pattern, ρ values are further plotted in Fig. 9c. Generally speaking, except for eastern Wyoming, northern Colorado, and northern California, the simulated SWE showed good correlation to the observation. As mentioned, the current simulation was conducted using one elevation band (for the efficiency of model calibration). With the increase of elevation bands in future simulations, the performance of snow simulation can be further improved.

The overall improvement from the computationally intensive calibration exercise is illustrated in Fig. 10. Focusing on Nash (Fig. 10a) and RMSE (Fig. 10b), the cumulative percentage of HUC8s is plotted. In terms of Nash, around 20 % of HUC8s ($\sim$ 450 HUC8s) are improved from less than 0.5 to greater than 0.5. In terms of RMSE, the modeling errors were on average reduced by $\sim 5\,\mathrm{mm\,yr^{-1}}$ for most of the HUC8s. While the best parameters at each HUC8 were identified, the performance of all examined combinations of parameters was also recorded to support further assessment. By calculating the sensitivity and trends of each parameter, it is hoped that the next model improvement can be achieved with fewer iterations and computational hours. In other words, the proposed hydrological dataset provides not only the currently best available parameters, but also the tested parameter sensitivity to support further fine calibration.

HESSD
10, 9575–9613, 2013

4 Summary and conclusion

This study introduces an effort to prepare a comprehensive hydrological model parameter dataset for large-scale, high-resolution climate change impact assessment. Several key inputs for hydrologic simulation, including meteorologic forcings, soil, land class, vegetation, and elevation, were collected and organized in refined 4 km grids. Using high performance computing, a spatially consistent calibration was performed for the VIC model. The VIC model simulation was driven by DAYMET daily meteorological forcing and was evaluated by USGS WaterWatch runoff observations for 2107 HUC8 Subbasins in the conterminous US. Overall, 1.5 million CPU-hours were used to develop a post-calibrated model parameter dataset to support fine-scale future hydro-climate assessments. The pre-organized model parameter dataset will be provided to interested parties to support further hydro-climate impact assessment. Although model calibration may yet be required for particular model applications, it is hoped the pre-organized dataset will help reduce the amount of effort needed for basic data preparation and organization. Depending on the specific needs, the parameter dataset can then be further calibrated effectively.

As a result of this exhaustive calibration exercise, it is now possible to more accurately estimate the resources required for further model improvement across the entire conterminous US. Calibrating a hydrologic model consistently for various watersheds can also increase understanding of the strengths and limitations of a particular hydrologic model across different climate regions. It can also help understand the best combination of hydrologic model and meteorological forcing dataset for specific regions. Although the extensive model calibration was performed for the VIC model, the computation and data framework were designed in a flexible manner so that other suitable hydrologic models could be incorporated in the future. By including multiple hydrologic model choices, we hope that it can provide flexibility for further applications and increase understanding of the modeling uncertainty associated with different hydrologic models in hydro-climate impact assessment.

HESSD
10, 9575–9613, 2013

Acknowledgements. This research was funded by the Laboratory Directed Research and Development (LDRD) Program of Oak Ridge National Laboratory, which is managed by UT-Battelle, LLC, for the US Department of Energy under Contract DE-AC05-00OR22725. The US Government retains a non-exclusive, paid-up, irrevocable, world-wide license to publish or reproduce the published form of this manuscript, or allow others to do so, for US Government purposes.

References

Abatzoglou, J. T.: Development of gridded surface meteorological data for ecological applications and modeling, Int. J. Climatol., 33, 121–131, doi:10.1002/joc.3413, 2013.

Ashfaq, M., Bowling, L. C., Cherkauer, K., Pal, J. S., and Diffenbaugh, N. S.: Influence of climate model biases and daily-scale temperature and precipitation events on hydrological impacts assessment: a case study of the United States, J. Geophys. Res., 115, D14116, doi:10.1029/2009JD012965, 2010.

Bohn, T. J., Podest, E., Schroeder, R., Pinto, N., McDonald, K. C., Glagolev, M., Filippov, I., Maksyutov, S., Heimann, M., and Lettenmaier, D. P.: The effects of surface moisture heterogeneity on wetland carbon fluxes in the West Siberian Lowland, Biogeosciences Discuss., 10, 6517–6562, doi:10.5194/bgd-10-6517-2013, 2013.

Bowling, L. C., Pomeroy, J. W., and Lettenmaier, D. P.: Parameterization of blowing-snow sublimation in a macroscale hydrology model, J. Hydrometeorol., 5, 745–762, doi:10.1175/1525-7541(2004)005<0745:POBSIA>2.0.CO;2, 2004.

Brakebill, J. W., Wolock, D. M., and Terziotti, S. E.: Digital hydrologic networks supporting applications related to spatially referenced regression modeling, J. Am. Water Resour. Assoc., 47, 916–932, doi:10.1111/j.1752-1688.2011.00578.x, 2011.

Cherkauer, K. A. and Lettenmaier, D. P.: Simulation of spatial variability in snow and frozen soil, J. Geophys. Res., 108, 8858, doi:10.1029/2003JD003575, 2003.

Cherkauer, K. A., Bowling, L. C., and Lettenmaier, D. P.: Variable Infiltration Capacity (VIC) cold land process model updates, Global Planet. Change, 38, 151–159, doi:10.1016/S0921-8181(03)00025-0, 2002.

HESSD

10, 9575–9613, 2013

Christensen, N. S., Wood, A. W., Voisin, N., Lettenmaier, D. P., and Palmer, R. N.: The effects of climate change on the hydrology and water resources of the Colorado river basin, Clim. Change, 62, 337–363, doi:10.1023/B:CLIM.0000013684.13621.1f, 2004.

Daly, C., Gibson, W. P., Taylor, G. H., Johnson, G. L., and Pasteris, P.: A knowledge-based approach to the statistical mapping of climate, Climate Res., 22, 99–113, doi:10.3354/cr022099, 2002.

Demaria, E., M., Nijssen, B., and Wagener, T.: Monte Carlo sensitivity analysis of land surface parameters using the Variable Infiltration Capacity model, J. Geophys. Res., 112, D11113, doi:10.1029/2006JD007534, 2007.

Farr, T. G., Rosen, P. A., Caro, E., Crippen, R., Duren, R., Hensley, S., Kobrick, M., Paller, M., Rodriguez, E., Roth, L., Seal, D., Shaffer, S., Shimada, J., Umland, J., Werner, M., Oskin, M., Burbank, D., and Alsdorf, D.: The Shuttle Radar Topography mission, Rev. Geophys., 45, RG2004, doi:10.1029/2005RG000183, 2007.

EPA (Environmental Protection Agency) and USGS (US Geological Survey): NHDPlus user guide, Environmental Protection Agency, available at: ftp://ftp.horizon-systems.com/NHDPlus/NHDPlusV1/documentation/NHDPLUSV1_UserGuide.pdf (last access: July 2013), 2010.

Gao, H., Tang, Q., Ferguson, C. R., Wood, E. F., and Lettenmaier, D. P.: Estimating the water budget of major US river basins via remote sensing, Int. J. Remote Sens., 31, 3955–3978, doi:10.1080/01431161.2010.483488, 2010.

Gesch, D., Oimoen, M., Greenlee, S., Nelson, C., Steuck, M., and Tyler, D.: The national elevation dataset, Photogramm. Eng. Remote Sens., 68, 5–11, 2002.

Govindaraju, R. S. and Rao, A. R.: Artificial neural networks: a passing fad in hydrology?, J. Hydrol. Eng., 5, 225–226, doi:10.1061/(ASCE)1084-0699(2000)5:3(225), 2000.

Hamlet, A. F. and Lettenmaier, D. P.: Effects of climate change on hydrology and water resources in the Columbia River basin, J. Am. Water Resour. Assoc., 35, 1597–1623, 1999.

Hansen, M., DeFries, R., Townshend, J. R. G., and Sohlberg, R.: Global land cover classification at 1 km resolution using a decision tree classifier, Int. J. Remote Sens., 21, 1331–1365, doi:10.1080/014311698214235, 2000.

Keane, R. E., Holsinger, L. M., Parsons, R. A., and Gray, K.: Climate change effects on historical range and variability of two large landscapes in western Montana, USA, Forest Ecol. Manag., 254, 375–389, doi:10.1016/j.foreco.2007.08.013, 2008.

HESSD
10, 9575–9613, 2013

Kimball, J. S., Running, S. W., and Nemani, R.: An improved method for estimating surface humidity from daily minimum temperature, Agr. Forest Meteorol., 85, 87–98, doi:10.1016/S0168-1923(96)02366-0, 1997.
Liang, X., Lettenmaier, D. P., Burges, S. J., and Wood, E. F.: A simple hydrologically based model of land surface water and energy fluxes for general circulation models, J. Geophys. Res., 99, 14415–14428, doi:10.1029/94JD00483, 1994.
Liang, X., Lettenmaier, D. P., and Wood, E. F.: Surface soil moisture parameterization of the VIC-2L model: evaluation and modification, Global Planet. Change, 13, 195–206, doi:10.1016/0921-8181(95)00046-1, 1996.
Lohmann, D., Raschke, E., Nijssen, B., and Lettenmaier, D. P.: Regional scale hydrology, Part 1: Formulation of the VIC-2L model coupled to a routing model, Hydrol. Sci. J., 43, 131–141, doi:10.1080/02626669809492107, 1998.
Maidment, D. R. (Ed.): Handbook of Hydrology, McGraw–Hill, New York, NY, 1993.
Manter, D. K., Reeser, P. W., and Stone, J. K.: A climate-based model for predicting geographic variation in Swiss needle cast severity in the Oregon coast range, Phytopathology, 95, 1256–1265, doi:10.1094/PHYTO-95-1256, 2005.
Maurer, E. P., Wood, A. W., Adam, J. C., and Lettenmaier, D. P.: A long-term hydrologically based dataset of land surface fluxes and states for the conterminous United States, J. Climate, 15, 3237–3251, doi:10.1175/1520-0442(2002)015<3237:ALTHBD>2.0.CO;2, 2002.
McCabe, G. J. and Hay, L. E.: Hydrologic effects of hypothetical climate change in the East River basin, Colorado, J. Hydrol. Sci., 40, 303–318, 1995.
Mesinger, F., DiMegoand, G., Kalnay, E., Mitchell, K., Shafran, P. C., Ebisuzaki, W., Jović, D., Woollen, J., Rogers, E., Berbery, E. H., Ek, M. B., Fan, Y., Grumbine, R., Higgins, W., Li, H., Lin, Y., Manikin, G., Parrish, D., and Shi, W.: North american regional reanalysis, B. Am. Meteorol. Soc., 87, 343–360, doi:10.1175/BAMS-87-3-343, 2006.
Mitchell, K. E., Lohmann, D., Houser, P. R., Wood, E. F., Schaake, J. C., Robock, A., Cosgrove, B. A., Sheffield, J., Duan, Q., Luo, L., Higgins, R. W., Pinker, R. T., Tarpley, J. D., Lettenmaier, D. P., Marshall, C. H., Entin, J. K., Pan, M., Shi, W., Koren, V., Meng, J., Ramsay, B. H., and Bailey, A. A.: The multi-institution North American Land Data Assimilation System (NLDAS): utilizing multiple GCIP products and partners in a continental distributed hydrological modeling system, J. Geophys. Res., 109, D07S90, doi:10.1029/2003JD003823, 2004.

HESSD
10, 9575–9613, 2013

Miller, D. A. and White, R. A.: A conterminous United States multilayer soil characteristics dataset for regional climate and hydrology modeling, Earth Interact., 2, 1–26, doi:10.1175/1087-3562(1998)002<0001:ACUSMS>2.3.CO;2, 1998.
Milly, P. C. D., Betancourt, J., Falkenmark, M., Hirsch, R. M., Kundzewicz, Z. W., Lettenmaier, D. P., and Stouffer, R. J.: Climate change: stationarity is dead: whither water management?, Science, 319, 573–574 , doi:10.1126/science.1151915, 2008.
Mote, P. W., Hamlet, A. F., Clark, M. P., and Lettenmaier, D. P.: Declining mountain snowpack in western North America, B. Am. Meteorol. Soc., 86, 39–49, doi:10.1175/BAMS-86-1-39, 2005.
Nijssen, B., Lettenmaier, D. P., Liang, X., Wetzel, S. W., and Wood, E. F.: Streamflow simulation for continental-scale river basins, Water Resour. Res., 33, 711–724, doi:10.1029/96WR03517, 1997.
Nijssen, B., O'Donnell, G. M., Lettenmaier, D. P., Lohmann, D., and Wood, E. F.: Predicting the discharge of global rivers, J. Climate, 14, 3307–3323, doi:10.1175/1520-0442(2001)014<3307:PTDOGR>2.0.CO;2, 2001.
Payne, J. T., Wood, A. W., Hamlet, A. F., Palmer, R. N., and Lettenmaier, D. P.: Mitigating the effects of climate change on the water resources of the Columbia River Basin, Clim. Change, 62, 233–256, 2004.
Schwarz, G. E. and Alexander, R. B.: State Soil Geographic (STATSGO) Data Base for the Conterminous United States, US Geological Survey, Reston, VA, 1995.
Seaber, P. R., Kapinos, F. P., and Knapp, G. L.: Hydrologic Unit Maps, US Geological Survey water supply paper 2294, 1987.
Shrestha, R., Tachikawa, Y., and Takara, K.: Input data resolution analysis for distributed hydrological modeling, J. Hydrol., 319, 36–50, doi:10.1016/j.jhydrol.2005.04.025, 2006.
Su, F., Adam, J. C., Bowling, L. C., and Lettenmaier, D. P.: Streamflow simulations of the terrestrial Arctic domain, J. Geophys. Res., 110, D08112, doi:10.1029/2004JD005518, 2005.
Thornton, P. E. and Running, S. W.: An improved algorithm for estimating incident daily solar radiation from measurements of temperature, humidity, and precipitation, Agr. Forest Meteorol., 93, 211–228, doi:10.1016/S0168-1923(98)00126-9, 1999.
Thornton, P. E., Running, S. W., and White, M. A.: Generating surfaces of daily meteorology variables over large regions of complex terrain, J. Hydrol., 190, 214–251, 1997.

HESSD
10, 9575–9613, 2013

White, M. A., Diffenbaugh, N. S., Jones, G. V., Pal, J. S., and Giorgi, F.: Extreme heat reduces and shifts United States premium wine production in the 21st century, P. Natl. Acad. Sci. USA, 103, 11217–11222, doi:10.1073/pnas.0603230103, 2006.
Wolock, D. M. and McCabe, G. J.: Explaining spatial variability in mean annual runoff in the conterminous United States, Climate Res., 11, 149–159, 1999.

HESSD
10, 9575–9613, 2013

Table 1. Selected VIC parameters for calibration.

Parameter	Range	Units	Description
b_{infilt}	0.001 ~ 0.8	N/A	Variable infiltration curve parameter
exp	8 ~ 30	N/A	Exponent of the Brooks–Corey drainage equation
$thick_2$	0.1 ~ 2	m	Thickness of soil layer 2
Ds	0 ~ 1	N/A	Fraction of the maximum velocity of baseflow where nonlinear baseflow begins
Ws	0.5 ~ 1.0	N/A	Fraction of maximum soil moisture where nonlinear baseflow occurs

HESSD
10, 9575–9613, 2013

Table 2. Matrices used for model calibration and evaluation.

Matrix	Name	Equation
R^2	Coefficient of determination	$\frac{\left[\sum_{t=1}^{n}(O_t-\overline{O})(Y_t-\overline{Y})\right]^2}{\left[\sum_{t=1}^{n}(O_t-\overline{O})^2\right]\left[\sum_{t=1}^{n}(Y_t-\overline{Y})^2\right]}$
Nash	Nash–Sutcliffe model efficiency coefficient	$1-\frac{\sum_{t=1}^{n}(O_t-Y_t)^2}{\sum_{t=1}^{n}(O_t-\overline{O})^2}$
MAE	Mean absolute error	$\frac{1}{n}\sum_{t=1}^{n}\lvert O_t-Y_t\rvert$
RMSE	Root mean square error	$\sqrt{\frac{1}{n}\sum_{t=1}^{n}(O_t-Y_t)^2}$

HESSD
10, 9575–9613, 2013

Table 3. Summary of median HUC8 matrices for each hydrologic region.

	Median statistics							
	Calibration period (1981–2000)				Validation period (2001–2008)			
	R^2	Nash	MAE ($mm\,yr^{-1}$)	RMSE ($mm\,yr^{-1}$)	R^2	Nash	MAE ($mm\,yr^{-1}$)	RMSE ($mm\,yr^{-1}$)
01 New England	0.843	0.826	12.2	17.8	0.829	0.810	14.4	21.2
02 Mid-Atlantic	0.825	0.798	9.8	14.3	0.824	0.746	11.1	15.4
03 South Atlantic-Gulf	0.830	0.807	10.0	14.2	0.813	0.705	10.9	14.8
04 Great Lakes	0.757	0.703	9.2	13.1	0.748	0.633	9.7	14.0
05 Ohio	0.849	0.824	10.4	14.9	0.865	0.823	10.8	14.6
06 Tennessee	0.809	0.776	12.5	16.9	0.815	0.766	12.7	17.8
07 Upper Mississippi	0.713	0.668	8.5	12.6	0.764	0.692	9.0	12.8
08 Lower Mississippi	0.774	0.704	16.7	23.4	0.744	0.596	17.8	24.9
09 Souris–Red–Rainy	0.488	0.416	3.6	6.3	0.421	0.269	4.9	8.1
10 Missouri	0.368	0.156	2.8	4.0	0.433	−0.296	2.7	3.5
11 Arkansas–White–Red	0.562	−0.006	8.9	12.2	0.596	−0.921	9.0	11.7
12 Texas Gulf	0.519	−0.442	11.1	14.8	0.573	−1.929	14.1	17.8
13 Rio Grande	0.078	−63.106	5.4	6.8	0.060	−56.580	5.2	6.4
14 Upper Colorado	0.339	0.113	5.0	6.6	0.409	−0.767	4.3	5.7
15 Lower Colorado	0.160	−12.028	7.2	9.0	0.130	−34.077	4.7	5.3
16 Great Basin	0.394	−0.183	6.1	8.0	0.415	−2.020	5.6	7.0
17 Pacific Northwest	0.669	0.527	15.2	21.3	0.652	0.478	13.3	18.2
18 California	0.702	0.590	9.6	17.1	0.689	0.255	8.4	14.4

HESSD
10, 9575–9613, 2013

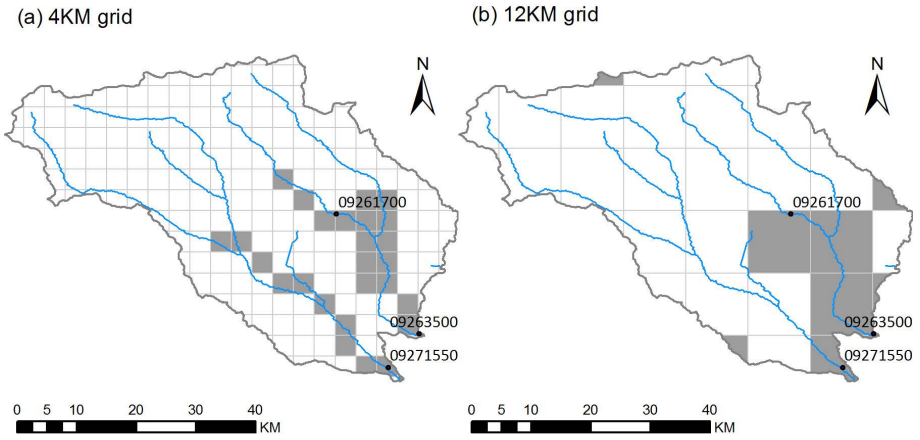

Fig. 1. Effect of spatial resolution in hydrologic modeling.

HESSD
10, 9575–9613, 2013

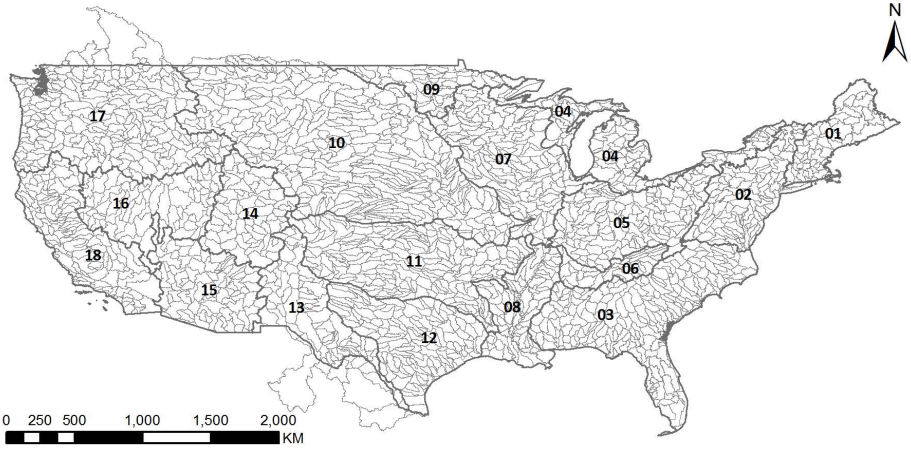

Fig. 2. Study area in this research. The smaller polygons represent the hydrologic Subbasins (HUC8) and the larger polygons with thicker grey boundaries represent the hydrologic Regions (HUC2). The 2-digit numbers represent the HUC2 ID.

HESSD
10, 9575–9613, 2013

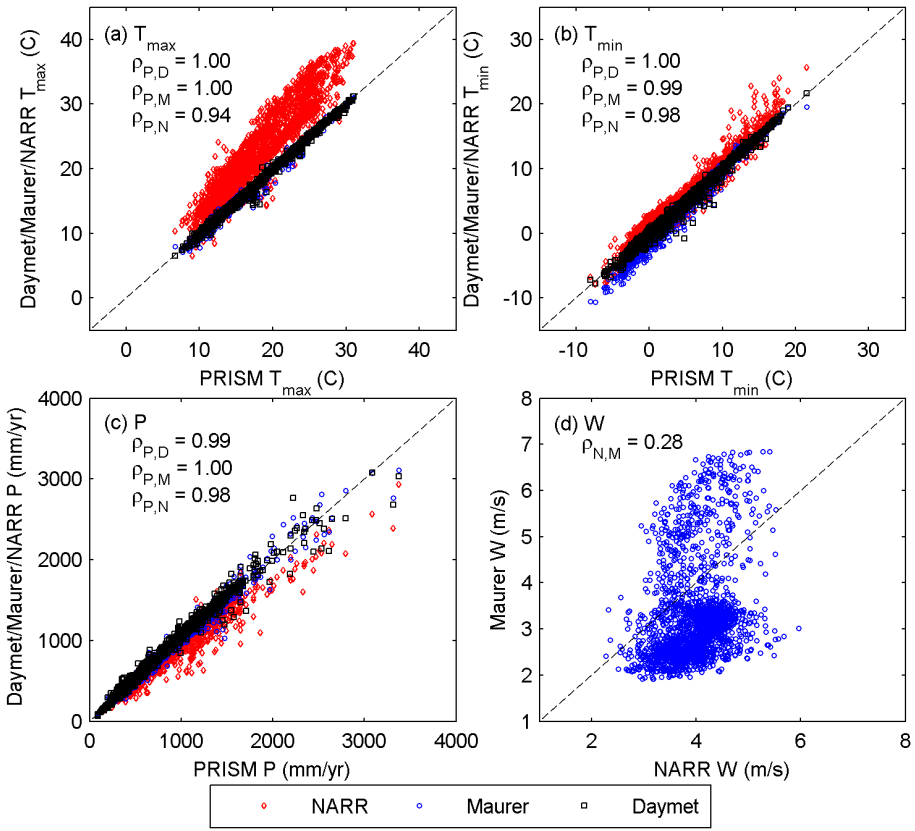

Fig. 3. Comparison among the 1980–2008 PRISM, DAYMET, Maurer, and NARR **(a)** mean daily maximum temperature T_{max}, **(b)** mean daily minimum temperature T_{min}, **(c)** annual total precipitation P, and **(d)** mean daily wind speed W. Each point represents the HUC8 annual average over the entire period.

HESSD
10, 9575–9613, 2013

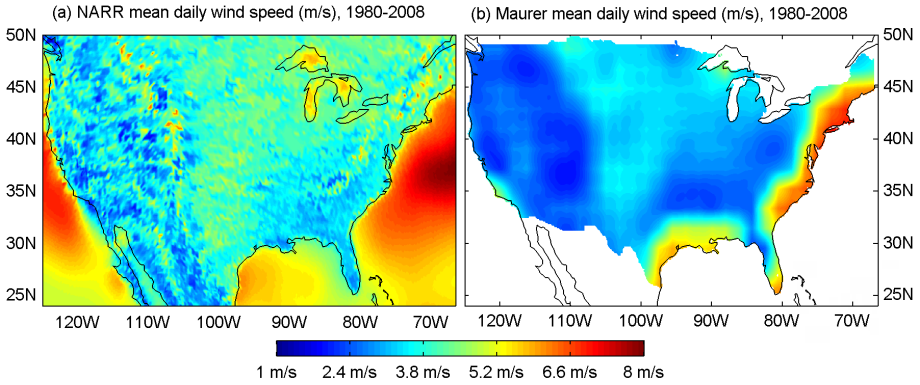

Fig. 4. Maps of mean daily wind speed.

HESSD
10, 9575–9613, 2013

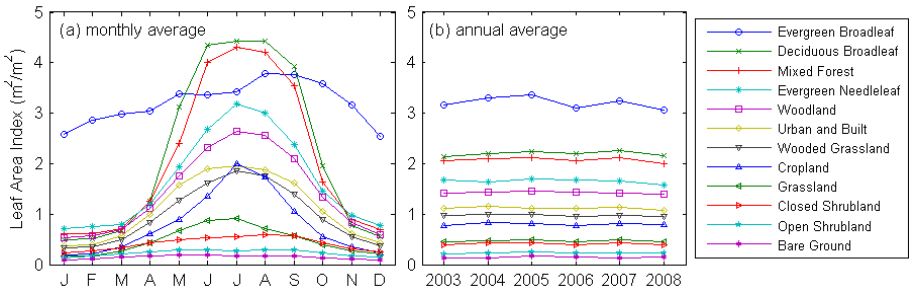

Fig. 5. The MODIS leaf area index summarized by the UMD land cover classification.

HESSD
10, 9575–9613, 2013

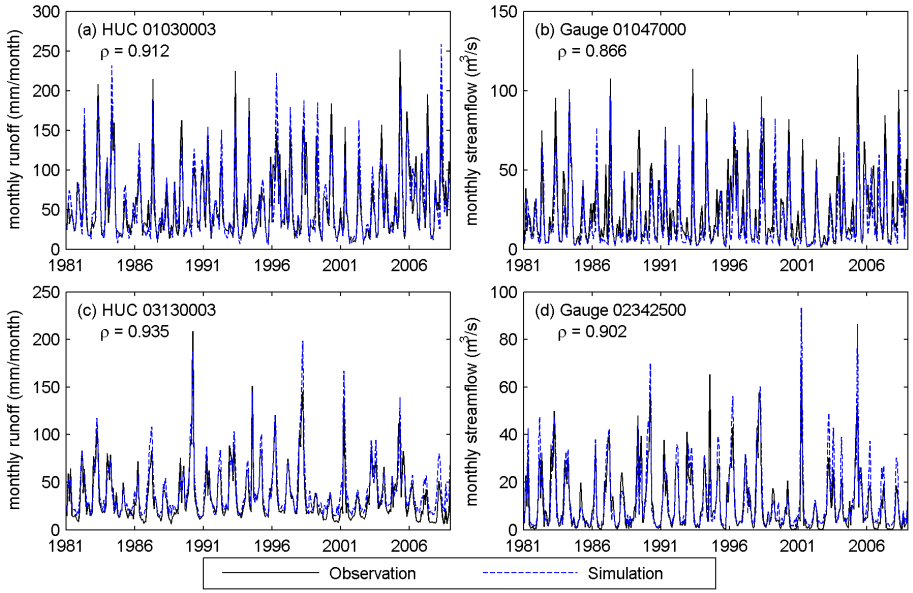

Fig. 6. The comparison between observed and simulated runoff (left panels) and observed and simulated streamflow (right panels). Gauge 01047000 is located at HUC01030003 and gauge 02342500 is located at HUC03130003.

HESSD
10, 9575–9613, 2013

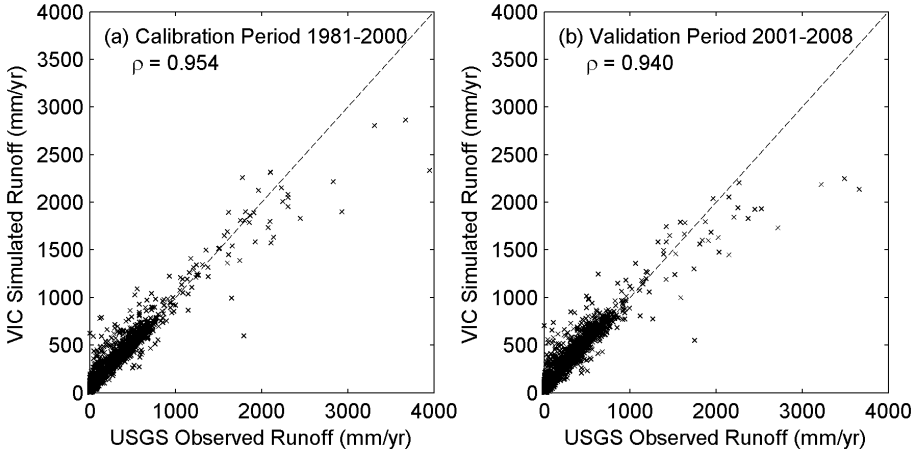

Fig. 7. The USGS WaterWatch observed runoff vs. the VIC simulated annual total runoff (surface runoff + baseflow) for both calibration and validation periods.

HESSD
10, 9575–9613, 2013

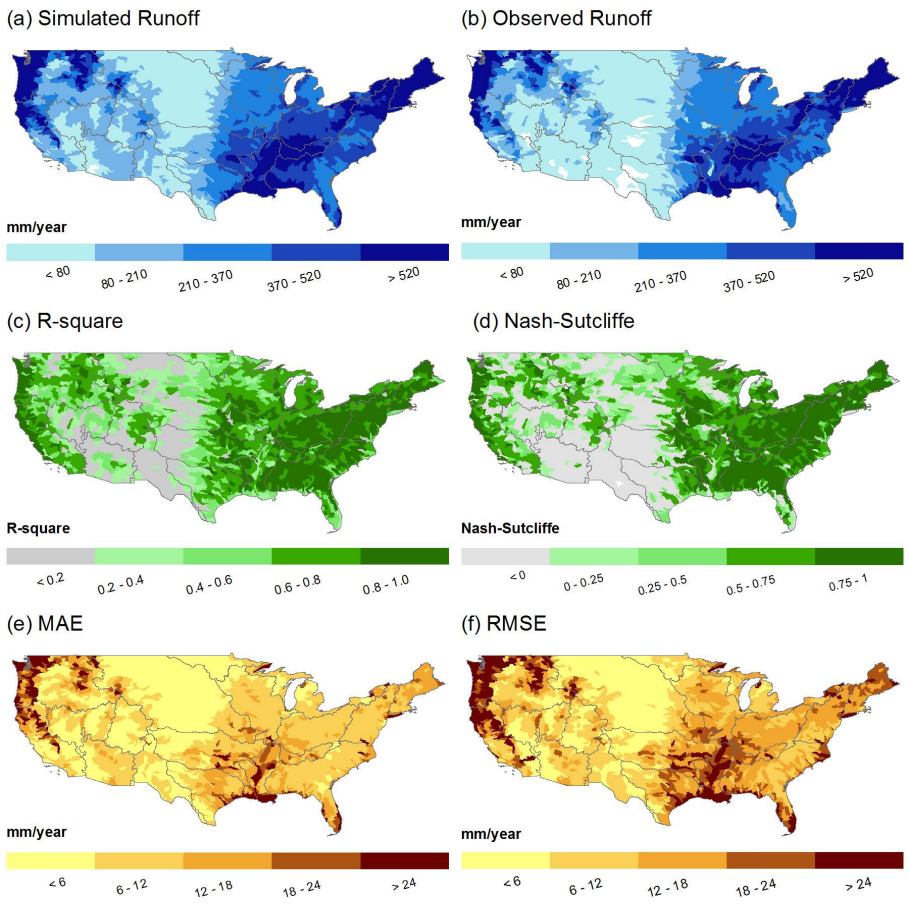

Fig. 8. Performance of calibrated VIC model at various HUC8s in the conterminous United States.

HESSD
10, 9575–9613, 2013

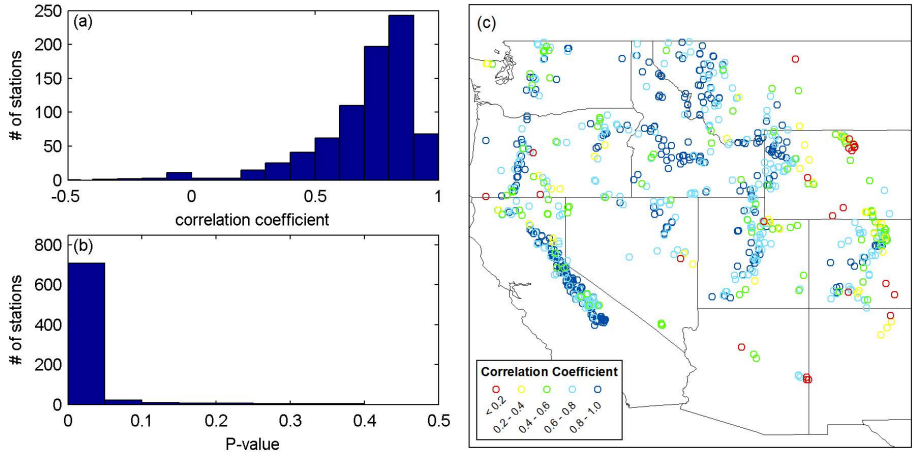

Fig. 9. Correlation coefficients between observed and simulated 1 April 1981–2000 snow water equivelant: **(a)** histogram of correlation coefficients from 784 selected stations, **(b)** histogram of *P* value, and **(c)** spatial pattern of correlation coefficients for all selected stations.

HESSD
10, 9575–9613, 2013

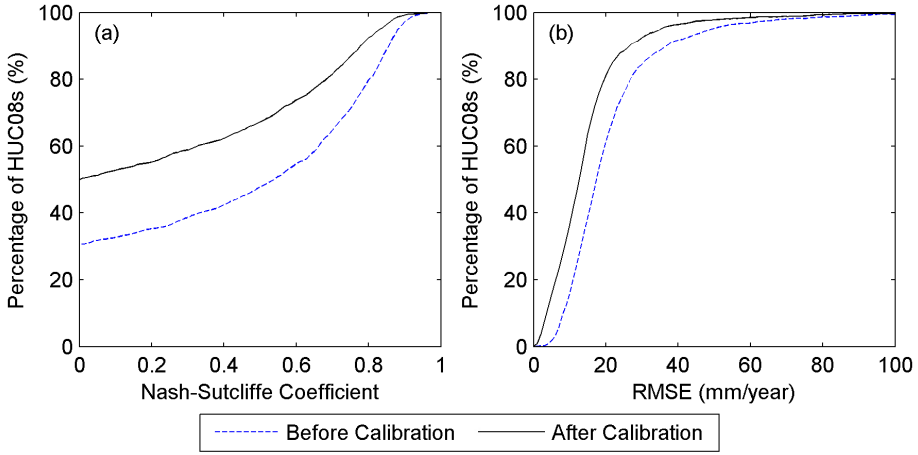

Fig. 10. Improvement of model performance before and after calibration.

HESSD
10, 9575–9613, 2013